79 GHz multilayer series-fed patch antenna array with stacked micro-via loading

Aliakbari Abar, Hanieh; Mosalanejad, Mohammad ; Soens, Charlotte ; Vandenbosch, Guy A. E. ; Lau, Buon Kiong

79 GHz Multilayer Series-Fed Patch Antenna Array with Stacked Micro-Via Loading

Hanieh Aliakbari, *Graduate Student Member, IEEE*, Mohammad Mosalanejad, Charlotte Soens, Guy A. E. Vandenbosch*, Fellow, IEEE*, and Buon Kiong Lau, *Fellow, IEEE*

Abstract—A wideband compact series-fed patch subarray is proposed for 79 GHz multiple-input multiple-output (MIMO) radar. The proposed subarray is, for the first time, loaded with stacked micro-vias (SMVs). Two sets of patches in the subarray are fed 180-degrees out-of-phase. A low-cost, high-resolution multilayer PCB technology, called "Any-Layer PCB", is used to implement the SMVs, which cannot be done by standard HDI PCB technology. Moreover, the technology supports small SMVs on different layers, hence thick machine-drilled vias can be avoided. For comparison, a series-fed patch subarray with no SMV loading is designed. It is shown that SMV loading facilitates a larger overlap of the impedance and gain bandwidths, leading to a larger operating bandwidth. The measured 10 dB impedance and 3 dB gain bandwidths are 15% and 9.6%, respectively. The sidelobe suppression is above 12.9 dB, and the maximum array gain is 12.67 dBi at 79.1 GHz. This subarray is suitable for MIMO radar, as its width is around 1/2-wavelength and the SMVs around it mitigate the crosstalk between the transmitting and receiving arrays.

Index Terms— Advanced multilayer PCB, 79 GHz, impedance bandwidth, series-fed patch array, stacked micro-vias loading.

I. INTRODUCTION

TO achieve high resolution for radar sensors the use of millimeter-wave (mm-wave) spectrum is essential [1]. Specifically, 77-81 GHz has been allocated for short/medium-range MIMO automotive radar sensors which are installed in cars to enable emergency braking, collision warning, blind-spot detection, and precrash vehicle preparation systems.

For radar designers, antenna arrays with compact structure, high efficiency, low sidelobe level (SLL) and ease of integration are very attractive [2]. Moreover, flat gain (e.g. by having a wider-than-specified impedance band) is desirable for automotive radar signal processing, as it gives designers more control over the transmit and receive filter design; alternatively, it offers higher range resolution [3], [4]. Wider bandwidth also increases the robustness of the prototype in covering the specified band amidst fabrication tolerances.

Different array topologies have been proposed for mm-wave automotive radar [5]-[14]. However, very few structures offer the above desired performance, while also fulfill practical requirements such as low-cost and mass reproducibility. For

H. Aliakbari and B. K. Lau are with the Department of Electrical and Information Technology (EIT), Lund University, 221 00 Lund, Sweden (E-mails: {hanieh.aliakbari_abar, buon_kiong.lau}@eit.lth.se).

M. Mosalanejad and C. Soens are with the Inter-University Microelectronics Center (IMEC), Leuven B-3001, Belgium (E-mails: mohammad.mosalanejad@esat.kuleuven.be, charlotte.soens@imec.be).

G. A. E. Vandenbosch is with the Electrical Engineering Department, KU Leuven, Leuven B-3001, Belgium (E-mail: guy.vandenbosch@ kuleuven.be).

example, the hybrid thin film design in [5] has efficiency below 40%, due to losses in the feeding network. In addition, it has high SLL levels in the E-plane and a limited beamwidth (i.e., 40°) in the H-plane, which is not suitable for automotive radars. The array-fed lens in [6] has narrow bandwidth (~5%). Low-temperature co-fired ceramic (LTCC) technology is used in [7], [8], but it is costly and unsuitable for mass production. Furthermore, the radiation efficiency of the array design in [7] is lower than 30%, due to the loss associated with the LTCC substrate materials. In [8], the patch array design uses WR12-to-laminated-waveguide transition in the feeding network, which is not compact and not attractive for automotive radars.

Microstrip patch antenna is suitable for array design in mm-wave automotive radar, as it is structurally simple, light weight, easy to fabricate at a low cost using printed circuit board (PCB) technology, and can be integrated in low-profile front ends [8]-[14]. In [9], parallel-fed patch array is designed using a standard PCB fabrication process. However, above 30 GHz, the losses in the feeding network of the parallel-fed patch arrays increase significantly, resulting in relatively low overall efficiencies (around 20%) [9]. Despite the broadband behavior of parallel-fed patch structures, series-fed structures are often used in patch array antennas for radar systems. This is because the lower complexity and loss of the feeding circuit are favorable for antenna gain enhancement in *E*-band. However, the impedance bandwidths of series-fed patch arrays are limited [10]-[18]. The patch array bandwidth can be improved either by modifying the patch element size [19] or shape [20]. This leads to improved bandwidth, but also degraded radiation performance across the band, due to added higher order modes. On the other hand, the radiation characteristics can be preserved by using only the fundamental array mode across the bandwidth and the impedance bandwidth can be improved by loading the entire array [21], or patches in parallel-fed array [22], at lower bands.

The focus of this work is to enhance the operating bandwidth of the fundamental mode of a series-fed patch array using vertical loading. For the first time, stacked micro-vias (SMVs) are loaded on the non-radiating edges of the patches to increase the array impedance bandwidth while preserving the array radiation characteristics. This design is visioned for 79 GHz automotive MIMO radar; however, the proposed bandwidth enhancement concept can be used for a general series-fed patch array in other applications/frequency bands. A prototype array, intended for integration as a subarray, has been fabricated with a low-cost "Any-Layer PCB" technology, which is suitable for mass production [4], [23]. As opposed to standard multilayer PCB technologies, the "Any-Layer PCB" technology can implement SMVs between layers.
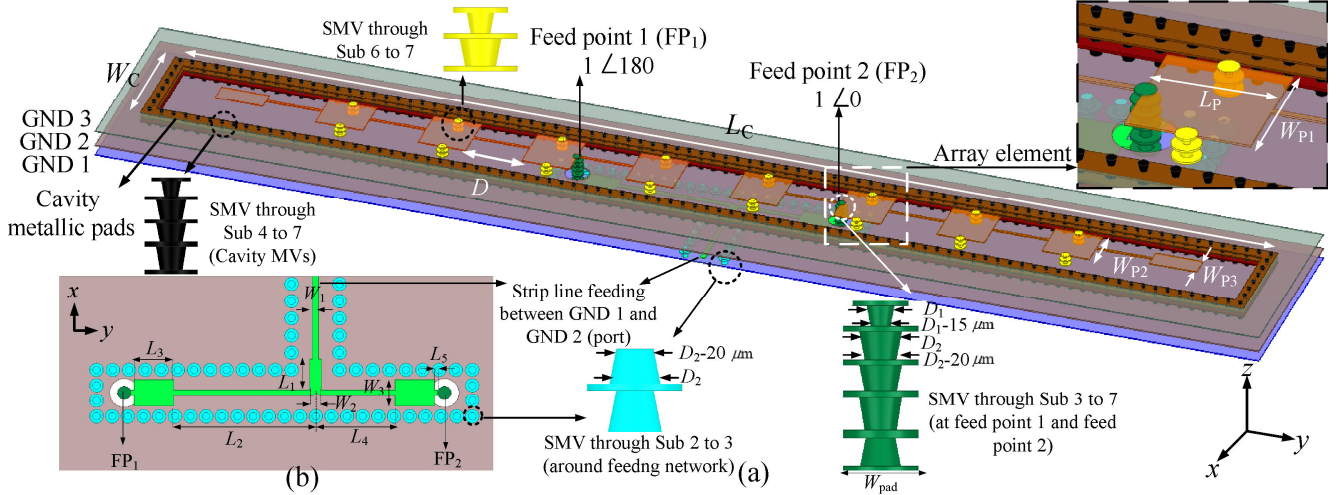
Fig. 1. (a) 3D view of series-fed patch antenna array and single patch element with four types of SMVs, and (b) feeding network at the bottom layer (GND 1 and Sub 1) is not shown for clarity. The corresponding layers are listed in Table I. Dimensions (mm): L_C = 22.5, W_C = 2.15, D = 1.16, W_{P1} = 1, W_{P2} = 0.85, W_{P3} = 0.4, L_P = 0.98, D_1 = 0.085, D_2 = 0.13, W_{pad} = 0.23, W_1 = 0.1, L_1 = 0.53, W_2 = 0.19, L_2 = 2.42, W_3 = 0.45, L_3 = 0.67, L_4 = 0.335, L_5 = 0.17.

II. Antenna Array Design

A. Single-element patch with SMVs

To design the series-fed patch antenna array on a multi-layer PCB, the first step is to design the array element. The enlarged version of an array element is shown in Fig. 1(a). The element is composed of a radiating rectangular patch, loaded by two SMVs (in yellow) on its non-radiating edges. It is noted that the SMVs in the design are small pieces of a metal (copper fillings) that can be used to connect a specific layer to every other layer, enabling very low metallic loss that can be neglected in normal circumstances. The electrical model of a single SMV can be broken into three sections, the upper pad, cone, and lower pad. Generally, similar to machine drilled vias, each section consists of both capacitance and inductance. At higher frequencies, the equivalent circuit of each section will become more distinct, i.e., the pads will mainly contribute to the capacitance (i.e., capacitor between the pads and GND, capacitor between pads), whereas the cone will contribute to the inductance. Thus, a single SMV can be approximated by a lumped equivalent circuit consisting of a series inductor and two parallel capacitors connected to the ground. The radiating patch is resonant, corresponding to the length (L_P) of $\lambda_g/2$ at 79 GHz (λ_g is the guided wavelength). The generic PCB used in this section has the same multi-layer substrate properties as given in Table I. The specific technology needed to realize the design involving the desired SMVs will be discussed in the next subsection.

Characteristic mode analysis (CMA) [24] of the array element is performed using 2019 Altair FEKO to explore the modal significance (MS) of the single patch's broadside fundamental mode (TM$_{01}$) around the resonant frequency. As Fig. 2(a) shows, the addition of the two SMVs in three layers has very little impact on the MS of the fundamental mode (> 0.7), as is the case for the characteristic currents and fields. However, the above-mentioned SMVs' equivalent circuit has a capacitance and inductance loading effect that can help to match the input impedance of the single element over a larger frequency band and increase the single series patch element's impedance bandwidth substantially, as shown in Fig. 2(b). The
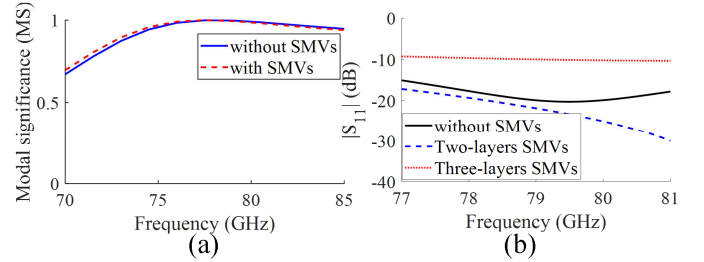

Fig. 2. (a) Modal significance of the single patch fundamental mode, (b) Impact of SMV loading in different layers on the reflection coefficient of a single patch.

exact change of the input impedance depends on the number of layers used by the SMVs (see Fig. 2(b)), which changes the equivalent capacitance and inductance of the SMVs' equivalent circuit. Consequently, the number of layers used by the SMVs should be optimized for the largest impedance bandwidth of the fundamental mode. For example, Fig. 2(b) shows that by adding two-layer SMVs, better matching and hence a larger impedance bandwidth is achievable. However, by using three-layer SMVs, the matching condition is degraded, indicating a smaller bandwidth. It is noted that the single patch simulation model in Fig. 1(a) is designed with two strip lines connected to its radiating edges, to prepare for the later array configuration. These lines are de-embedded from the $|S_{11}|$ in Fig. 2(b). The next step is to choose a technology to implement SMVs in the array, which is suitable for E-band.

B. SMV Implementation challenge

The via process was not mature before 2000. Specifically, stacked vias was extremely challenging for fabrication, or even impossible to fabricate, and would increase drastically the final cost of the antenna while spoiling its reliability [25].

Furthermore, as a result of physically small wavelengths, fabrication tolerances are severe in the mm-wave band, especially at higher frequencies. Thus, accurate and cost-efficient fabrication processes are needed in this band to embed mass-producible antennas in multilayer substrates. To realize the antenna and SMVs in this work, a new PCB technology, called "advanced Any-Layer PCB", is used [4], [23]. The fundamental technical advancement of the "Any-Layer PCB"
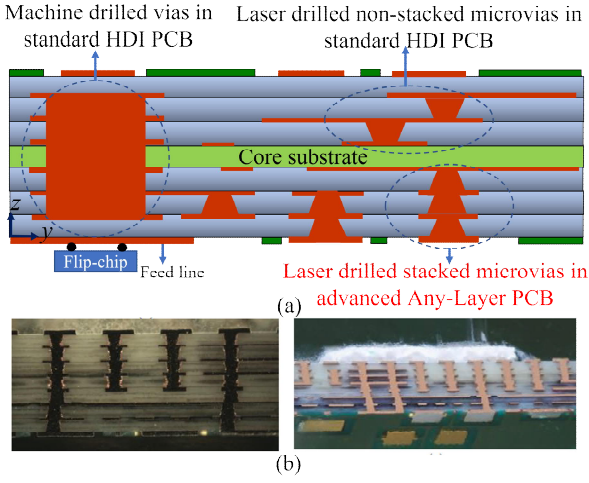
Fig. 3. (a) Different implementation of vias, (b) the SMVs implemented in "Any-Layer PCB" technology (cross section views).

over standard high-definition interconnect (HDI) PCB technology [26], is that stacking micro-vias is possible. This facilitates the possible connection of a specific layer to every other layer within the PCB build-up (see Fig. 3). Thus, the huge restriction that the laser-drilled micro-vias used in the HDI PCB design process cannot be stacked is removed. Moreover, conventionally drilled, blind, or through-hole vias created by machine drilling (see Fig. 3) deliver minimum hole and pad sizes of 200 and 400 μm, respectively. These dimensions are not suitable for high resolution and higher routing density in PCBs designed for E-band. For laser-drilled micro-vias in "Any-Layer PCB" technology, these values are smaller (i.e., 75 and 175 μm), enabling higher routing density and more compact final PCBs.

LTCC technology can also realize small stacked vias in mm-wave, but the cost is higher than standard multilayer PCB fabrication. Higher dielectric constant of LTCC materials and higher cost for mass production with respect to any-layer PCB makes LTCC technology less attractive [27]. It is noted that the "Any-layer PCB" technology has been used before, e.g., [4], [23]. However, this was the first time to use this benefit of the "Any-Layer PCB" in the design process.

C. Series-fed patch array with SMVs in "Any-Layer PCB"

The proposed SMV-loaded series-fed array of microstrip patches are illustrated in Fig. 1(a). It consists of two sets of patches, each with five SMVs loaded patch elements described in Section II-A. The two sets of five resonant patches are fed by two SMVs and two transmission lines that provide 180° phase difference of the input signal, which are equally split (using a power splitter made from strip lines and matching quarter wave lines) from a single transmission line (see Fig. 1(b)). The length of the inter-connecting lines between the patches must be $\lambda_g/2$. The widths of the two patches at each outer end of the array are optimized to achieve the desired radiation conductance and to retain bandwidth [28]. Four types of SMVs (shown in four different colors in Fig. 1(a)) are used in the array to connect different layers. The dimension and the direction (i.e., larger diameter at the top or bottom) of each cone-shaped micro-via within a given SMV depend on the layer in which it is placed, as depicted for the green SMV in Fig. 1(a). Metallic pads (see

TABLE I
ANY-LAYER HDI PCB BUILDUP

| Material	Dielectric constant	Tangent delta	Thickness (um)
Copper layer 8 (patch array, cavity pad)			16
Sub7: Prepreg	3.26	0.01	68
Copper layer 7 (GND 3, cavity pad)			16
Sub6: Prepreg	3.22	0.01	104
Copper layer 6 (Signal, cavity pad)			16
Sub5: Prepreg	3.22	0.01	104
Copper layer 5 (Signal, cavity pad)			16
Sub4: Laminate core	3.37	0.01	100
Copper layer 4 (GND 2-two feeding holes)			23
Sub3: Prepreg	3.22	0.01	104
Copper layer 3 (Feeding network)			16
Sub2: Prepreg	3.22	0.01	104
Copper layer 2 (GND 1)			16
Sub1: Prepreg	3.25	0.01	68
Copper layer 1 (Signal)			23
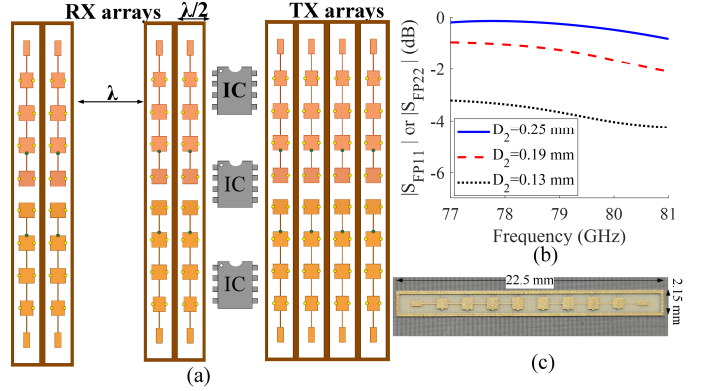
Fig. 4. (a) 4 × 4 MIMO medium-range automotive radar module, (b) Impact of wider loading SMVs on the reflection coefficient of an array before adding the matching network and splitter in Fig. 1(b) (i.e., $|S_{FP11}|$ or $|S_{FP22}|$), (c) fabricated prototype in advanced Any-Layer PCB technology.

Fig. 1(a)) are used to improve the electrical contact of the micro-vias stacked on different layers. The loading SMVs connect layers 8 to 6 within the PCB build-up in Table I. The two feeding SMVs connect the patches in layer 8 to the two endpoints of the power splitter embedded in layer 3.

Since three ground planes (GND 1, 2, 3) are used in the build-up in Table I, there is a potential for the excitation of parallel-plate modes and surface waves. Thus, the antenna array is surrounded by a metallic cavity, implemented by SMVs connecting layer 8 to 4. The SMVs that are around the strip lines of the power splitter connect layer 2 to 4. The metallic walls significantly suppress the crosstalk between the transmitting and receiving arrays upon integration into a MIMO module and they do not change the array radiation pattern. In addition, the cavity width is very close to $\lambda_0/2$ at 79 GHz, which suppresses sidelobes in the MIMO array. To our knowledge, no existing design (e.g., [5]-[11]) fulfills these MIMO radar requirements. Figure 4(a) shows an example of a MIMO radar module, which realizes the virtual array concept in the receiving end.

Similar to Section II-A, CMA is performed for the array with and without the SMV loading in Fig. 1(a), before adding the matching section in Fig. 1(b). Again, the MS curves in Fig. 5(a) show that the bandwidth of the array fundamental mode is not affected. However, as before, SMVs enable less impedance change over the frequency band, which corresponds to a larger intrinsic impedance bandwidth (see Fig. 5(b)).

Finally, the reflection coefficient of the array for different SMV sizes (D_2 in Fig. 1(a)) is plotted for the same band in Fig.
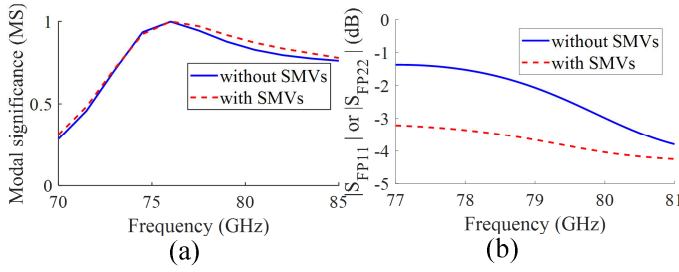
Fig. 5. (a) Modal significance of the fundamental mode of an array, (b) Impact of SMVs on the reflection coefficient of an array before adding matching network and splitter in Fig. 1(b) (i.e., S_{FP11} or S_{FP22}).
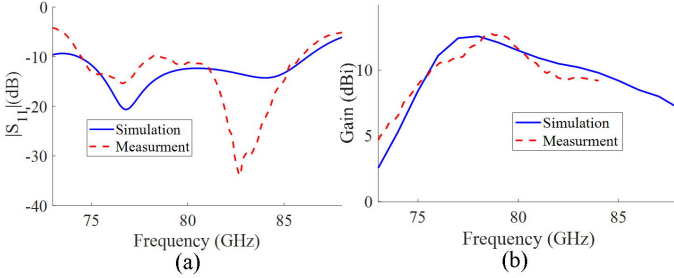

Fig. 6. Simulated and measured array (a) $|S_{11}|$ and (b) gain versus frequency.

4(b). D_1 is set to $D_1 = D_2 - 0.045$ mm. Figure 4(b) shows that, by making the SMV diameter wider, the intrinsic impedance bandwidth degrades, which complicates matching and reduces achievable impedance bandwidth.

By increasing the SMV size, the total equivalent capacitance of the SMVs will increase. This is because the surface area of the via is increasing and capacitance is proportional to the surface area. Thus, the reactance part of the input impedance will increase, which makes the input impedance harder to match. It is noted that the area of the pad in machine-drilled vias is about four times the pad areas in SMVs. This highlights the matching benefit of the SMVs provided by the "Any-Layer PCB" technology, which cannot be realized with machine-drilled vias. Figure 4(c) shows the fabricated prototype of the series fed patch with SMVs using the "Any-Layer PCB" technology.

III. MEASUREMENT

The simulated and measured results of reflection coefficient magnitude ($|S_{11}|$) and gain of the array in Fig. 4(c) are shown in Fig. 6. The measured $|S_{11}|$ is lower than -10 dB for 74.50-85.81 GHz (15%). The measured maximum gain is 12.67 dB at 79.1 GHz and the 3 dB gain bandwidth is 75.4-83 GHz. Furthermore, the maximum gain drop is less than 0.8 dB within 77–81 GHz. This flat-gain behavior with matched condition is attractive for radar designers [1]. The discrepancies between the simulated and measured results are mainly due to fabrication tolerances in the geometrical and material parameters in this technology. These tolerances are unavoidable, especially in multilayer PCB and at high frequencies [15]. The simulated total radiation efficiency of the full array including the feeding losses is 63%.

The setup in [23] was used to measure the radiation pattern. In Fig. 7, the simulated and measured patterns are shown at 76, 79 and 83 GHz. The simulated and measured SLL are under -16.4 dB and -12.9 dB, respectively, for all frequencies. Considering the reflection loss, 3 dB gain bandwidth, and SLL, this antenna can be used for 75.4-83 GHz (9.6% bandwidth).
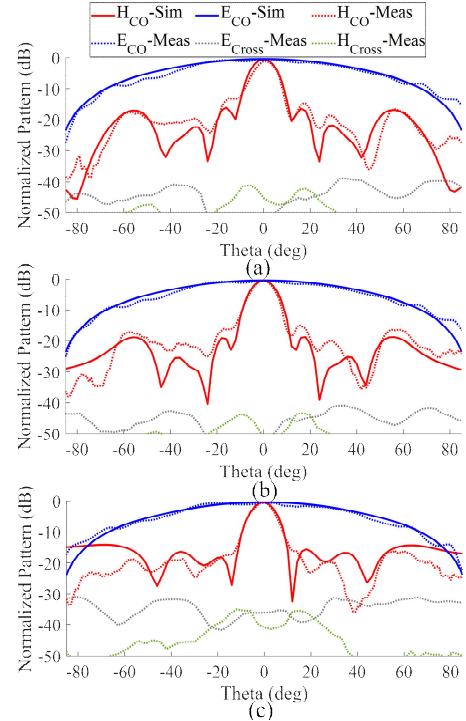

Fig. 7. Simulated (Sim) and measured (Meas) radiation patterns at (a) 76, (b) 79 and (c) 83 GHz.

TABLE II
COMPARISON OF SOME RECENT MM-WAVE SERIES-FED PATCH ARRAYS

Ref.	Frequency (BW)	Gain	Gain variation	Efficiency	Array architecture
[14]	77 GHz (6%)	20 dB	>2 dB	66%	6×10 (1×10 series fed subarrays)
[10]	79 GHz (5%)	22 dB	2.5 dB	NA	8×6 (1×6 series fed subarrays)
[18]	24 GHz (3%)	18 dB	NA	NA	8×8 (1×8 series fed subarrays)
[13]	77 GHz (4%)	15 dB	>1.5 dB	NA	1×16 series fed subarray
This Work	**79 GHz (9.6%)**	**12.67 dB**	**0.8 dB**	**63%**	**1×10 series fed subarray**

The measured 3 dB beamwidths in azimuth and elevation are 72° and 12°, respectively, which satisfy the requirements for automotive radars [1]. Finally, a comparison of the proposed design with other mm-wave series-fed patch arrays is given in Table II. The proposed design offers a notably larger impedance bandwidth and very stable gain within the band. As expected, the array gain is proportionally higher for larger arrays.

IV. CONCLUSION

A novel compact patch antenna array loaded with SMVs has been presented. The SMV loading enables an array topology with wide combined impedance-gain bandwidth. The proposed array has been realized by the low-cost high resolution "Any-Layer PCB" technology. This technology has a unique feature that allows the designer to distribute stacked and staggered vias. The small size SMVs compared to machine drilled vias facilitates a more compact antenna by enabling the implementation of a compact structure using vertical configuration. The proposed series-fed patch array topology is a good candidate for 79 GHz MIMO automotive radar due to the low cost, compact size, ability to suppress surface waves, as well as relatively wide impedance and flat-gain bandwidths.

REFERENCES

[1] J. Hasch, E. Topak, R. Schnabel, T. Zwick, R. Weigel, and C. Waldschmidt, "Millimeter-wave technology for automotive radar sensors in the 77 GHz Frequency Band," *IEEE Trans. Microw. Theory Techn.*, vol. 60, no. 3, pp. 845–860, Mar. 2012.

[2] S. Yoo, Y. Milyakh, H. Kim, C. Hong, and H. Choo, "Patch array antenna using a dual coupled feeding structure for 79 GHz automotive radar applications," *IEEE Antennas Wireless Propag. Lett.*, vol. 19, pp. 676-679, 2020.

[3] F. Bauer, and W. Menzel, "A 79-GHz planar antenna array using ceramic-filled cavity resonators in LTCC," *IEEE Antennas Wireless Propag. Lett.*, vol. 12, pp. 910-913, 2013.

[4] M. Mosalanejad, I. Ocket, C. Soens, and G. A. E. Vandenbosch, "Multilayer compact grid antenna array for 79 GHz automotive radar applications," *IEEE Antennas Wireless Propag. Lett.*, vol. 17, pp. 1677-1681, 2018.

[5] O. Khan, J. Meyer, K. Baur, and C. Waldshmidt, "Hybrid thin film antenna for automotive radar at 79 GHz," *IEEE Trans. Antennas Propag.*, vol. 65, no. 10, pp. 5076-5085, Oct. 2017.

[6] P. Hallbjorner, Z. He, S. Bruce, and S. Cheng, "Low-profile 77-GHz lens antenna with array feeder," *IEEE Antennas Wireless Propag. Lett.*, vol. 11, pp. 205-207, 2012.

[7] F. Bauer and W. Menzel, "A 79-GHz resonant laminated waveguide slotted array antenna using novel shaped slots in LTCC," *IEEE Antennas Wireless Propag. Lett.*, vol. 12, pp. 296-299, 2013.

[8] X. Wang and A. Stelzer, "A 79-GHz LTCC patch array antenna using a laminated waveguide-based vertical parallel feed," *IEEE Antennas Wireless Propag. Lett.*, vol. 12, pp. 987–990, 2013.

[9] Y. J. Cheng, Y. X. Gui, and Z. G. Liu, "W-band large-scale high-gain planar integrated antenna array," *IEEE Trans. Antennas Propag.*, vol. 62, no. 6, pp. 3370-3373, Jun. 2014.

[10] Y. Liu, G. Bai, and M. Yagoub. "A 79GHz series fed microstrip patch antenna array with bandwidth enhancement and sidelobe suppression," in *Proc. IEEE Int. Conf. Radar Antenna Microw. Electron. Telecommun. (ICRAMET)*, Tangerang, Indonesia, Nov 18-20, 2020.

[11] I, Aziz, W.C. Liao, H. Aliakbari, and W. Simon. "Compact and low-cost linear antenna array for millimeter wave automotive radar applications," in *Proc. 14th Europ. Conf. Antennas Propag. (EuCAP)*, Copenhagen, Denmark, Mar. 15-20, 2020, pp. 1–4.

[12] J. R. James and P. S. Hall, *Handbook of Microstrip Antennas* (IEE Electromagnetic Waves Series). London, U.K.: Peter Peregrinus, vol. 2, 1989.

[13] J. Yan, H. Wang, J. Yin, C. Yu, and W. Hong, "Planar series-fed antenna array for 77 GHz automotive radar," in *Proc. 6th Asia-Pacific Conf. Antennas Propag.*, Xi'an, China, 2017, pp. 1–3.

[14] J. Xu, W. Hong, H. Zhang, G. Wang, Y. Yu, and Z. H. Jiang "An array antenna for both long- and medium-range 77 GHz automotive radar applications," *IEEE Trans. Antennas. Propag,* vol. 65, no. 12, pp. 7207-7216, Dec 2017.

[15] T. Yuan, N. Yuan, and L. W. Li, "A novel series-fed taper antenna array design," *IEEE Trans. Antennas Propag.*, vol. 7, pp. 362-365, 2008.

[16] N. Ojaroudiparchin, M. Shen, S. Zhang, and G. F. Pedersen, "A switchable 3-D-coverage-phased array antenna package for 5G mobile terminals," *IEEE Antennas Wireless Propag. Lett.*, vol. 15, no. 11, pp. 1747-1750, 2016.

[17] V. Semkin, *et al*., "Beam switching conformal antenna array for mm-wave communications," *IEEE Antennas Wireless Propag. Lett.*, vol. 15, pp. 28-31, 2016.

[18] K. Wincza, and S. Gruszczynski "Microstrip antenna arrays fed by a series-parallel slot-coupled feeding network," *IEEE Antennas Wireless Propag. Lett.*, vol. 10, pp. 991-994, 2011.

[19] Y. Luo, Z. N. Chen and K. Ma, "A single-layer dual-polarized differentially fed patch antenna with enhanced gain and bandwidth operating at dual compressed high-order modes using characteristic mode analysis," *IEEE Trans. Antennas. Propag,* vol. 68, no. 5, pp. 4082-4087, May 2020.

[20] J. Y. Sze and K. L. Wong, "Slotted rectangular microstrip antenna for bandwidth enhancement," *IEEE Trans. Antennas Propag.*, vol. 48, no. 8, pp. 1149-1152, Aug. 2000.

[21] P. C. Stickland, "Series-fed microstrip patch arrays with periodic loading," *IEEE Trans. Antennas Propag.*, vol. 43, no. 12, pp. 1472-1474, Dec. 1995.

[22] L. Han, and K. Wu. "24-GHz bandwidth-enhanced microstrip array printed on a single-layer electrically-thin substrate for automotive applications," *IEEE Trans. Antennas Propag.*, vol. 60, pp. 2555-2558, Dec. 2012.

[23] H. Aliakbari, M. Mosalanejad, C. Soens, G. A. E. Vandenbosch, and B. K. Lau, "Wideband SIW-based low-cost multilayer slot antenna array for E-band applications," *IEEE Trans. Compon., Packag., Manuf., Technol.*, vol. 9, no. 8, pp. 1568-1575, 2019.

[24] R. Harrington and J. Mautz, "Theory of characteristic modes for conducting bodies," *IEEE Trans. Antennas Propag.*, vol. AP-19, no. 5, pp. 622-628, Sep. 1971.

[25] T. Potelon, M. Ettorre, L. Le Coq, T. Bateman, J. Francey, and R. Sauleau, "Reconfigurable CTS antenna fully integrated in PCB technology for 5G backhaul applications", *IEEE Trans. Antennas Propag.*, vol. 67, no. 6, pp. 3609-3618, Jun. 2019.

[26] AT&S, "HDI microvia PCBs." [Online]. Available: https://ats.net/ products-technology/product-portfolio/hdi-microvia-pcbs/

[27] F. F. Manzillo, M. Ettorre, M. S. Lahti, K. T. Kautio, D. Lelaidier, E. Seguenot, and R. Sauleau, "A multilayer LTCC solution for integrating 5G access point antenna modules", *IEEE Trans. Microw. Theory Tech.*, vol. 64, no. 7, pp. 2272-2283, Jul. 2016.

[28] S. Sengupta, D. R. Jackson, and S. A. Long, "A method for analyzing a linear series-fed rectangular microstrip antenna array," *IEEE Trans. Antennas Propag.*, vol. 63, no. 8, pp. 3731-3736, Aug. 2015.